Journal of the Korean Physical Society, Vol. 76, No. 10, May 2020, pp. 916∼922

Investigation of the Mechanical, Electronic and Phonon Properties of X_2ScAl (X = Ir, Os, and Pt) Heusler Compounds

Nihat Arikan*
Department of Mathematics and Science, Kırşehir Ahi Evran University, Kırşehir 40100, Turkey

Hamza Yaşar Ocak
Department of Physics, Kütahya Dumlupınar University, Kütahya 43100, Turkey

Gökçen Dikici Yildiz
Department of Physics, Kırıkkale University, Kırıkkale 71450, Turkey

Yasin Göktürk Yildiz†
Department of Electronics and Otomation, Kırıkkale University, Kırıkkale 71450, Turkey

Rahmi Ünal
Department of Mechanical Engineering, Gazi University, Ankara 06560, Turkey

(Received 4 December 2019; revised 8 March 2020; accepted 9 March 2020)

In the present study, the second-order elastic constants and the electronic band structures of the X_2ScAl (x = Ir, Os, and Pt) compounds crystallized in the $L2_1$ phase were calculated separately by using the *ab-initio* density functional theory. According to the results for the second-order elastic constants, these compounds met the Born mechanical stability criteria. Also, according to the Pugh criteria, they were found to have a ductile structure and to show anisotropic behavior. The microhardneses of the compounds were between 2 and 14 GPa, and the highest hardness was found in the Ir_2ScAl (14.290 GPa) compound. In addition, the energy band structures of these compounds were calculated, and the crystals were found to have a metallic bond structure. All the computed data were compared with previously calculated results obtained with different methods. According to the findings obtained in the present study, in terms of its mechanical and electronic behaviors, Ir_2ScAl was found to have better physical properties than Os_2ScAl and Pt_2ScAl. The phonon dispersion curves and their corresponding total and projected densities of states were investigated for the first time by using a linear-response approach in the context of density functional perturbation theory. The frequencies of the optical phonon modes of all compounds at the Γ point were 4.767, 7.504 and 9.271 THz for Ir_2ScAl, 2.761, 7.985 and 9.184 THz for Os_2ScAl and 2.012, 5.6952 and 8.118 THz for Pt_2ScAl. The heat capacity C_v at constant volume versus temperature was calculated using a quasi-harmonic approach and the results are discussed.

PACS numbers: 62.20.−x, 31.15.E−, 71.20.−b, 63.20.D−
Keywords: Heusler compounds, Mechanical properties, DFT, Electronic band structure, Phonon
DOI: 10.3938/jkps.76.916

I. INTRODUCTION

The Heusler compounds discovered by Fritz Heusler are of great interest due to their rich physical properties, such as ferromagnetism, shape memory, semi-metal behavior and thermoelectric properties [1]. Furthermore, these properties can be regulated by varying the components of the material or the proportions of the components [2]. Heusler compounds comprise a remarkable class of intermetallic materials of 1:1:1 (commonly referred to as semi-Heusler) or 2:1:1 compounds with more than 1500 species. Today, more than a century after their first discovery by Fritz Heusler, they are still an active field of research. New properties and potential application areas have been continuously discovered for these compounds. Estimating of topological insulators is the latest example for these studies [3].

The Heusler compounds are represented by the for-

*E-mail: narikan@ahievran.edu.tr
†E-mail: gokturk@kku.edu.tr

mula X_2YZ and are ternary intermetallic compounds with the $L2_1$ crystal structure. In general, X and Y are transition metals while Z is a major group element. Numerous important factors determine the formation of intermetallic compounds. For instance, atomic size plays a decisive role because any atom must meet the spatial requirement of the given structure type. In their study, Gillessen and Dronskowski [4] calculated the crystallographic parameters of the Heusler phases formed with iron and platinum group metals. In this context, they selected Fe, Co, Ni, Ru, Rh, Pd, Os, Ir, and Pt as X elemental, Sc, Ti, V, Cr, Mn, Fe, Co, Ni, Cu and Zn as Y elemental, and Al, Ga, In, T1, Ge, Sn, Pb, Sb, and Bi as the placeholder Z atoms. In addition, the same researchers tried to determine which compounds could be synthesized most easily with negative formation enthalpies for experimental studies.

The researchers have reported that only 12% of 810 X_2YZ potential Heusler compounds have been described experimentally so far and, therefore can be found in crystallographic databases. The values of the elastic constants of the Ir_2ScAl and the Pt_2ScAl compounds were obtained by using VASP-GGA calculations [5]. In the literature, studies determining the descriptive properties of Heusler compounds, such as phase transitions, thermodynamic stability, and transport are insufficient. The lattice parameters and the formation enthalpies of Os_2ScAl and Pt_2ScAl compounds have been examined theoretically [6]. In addition, Gillessen [7] calculated the theoretical parameters for X_2ScAl (X = Ir, Os, and Pt) compounds.

The present work focused on the theoretical study of the structural, electronic, thermodynamic and elastic properties of X_2ScAl (X = Ir, Os, and Pt) compounds and on the phonon properties by using the density functional perturbation theory (DFPT). Phonon properties are necessary for a microscopic understanding of lattice dynamics. Information from the phonon spectrum plays an important role in determining various material properties, such as phase transitions, thermodynamic stability, and heat properties. This study aimed use density functional theory to determine the structural, electronic, elastic and phonon properties of these compounds.

II. METHOD

In the present study, the calculations made to investigate the basic properties of X_2ScAl (X = Ir, Os and Pt) compounds were performed using a plane-wave pseudopotential scheme in density-functional theory (DFT) utilizing the Quantum-ESPRESSO package [8] program. The electronic exchange-correlation potential was calculated by using the generalized slope approximation (GGA) parameterized by Perdew, Burke, and Ernzerhof (PBE) [9]. The wave functions were expanded in the plane-wave basis sets determined by a 40 Ry kinetic energy interruption and a $10 \times 10 \times 10$ **k**-point mesh was used for the Brillouin-zone integrations. The electronic charge density was evaluated up to a kinetic energy cut-off 400 Ry. The convergence threshold was taken a 10^{-9} Ry with a mixing beta of 0.7 so that the results would be appropriately precise. With the smearing technique, we usual a smearing parameter [10] of σ = 0.02 Ry for integration below the Fermi surface. To obtain self-agreement solutions of the Kohn-Sham equations, we calculated the lattice dynamics properties according to the DFPT [11,12]. In order to find the phonon dispersion curves and the densities of states along all the symmetry directions, we calculated eight dynamic matrices on a $4 \times 4 \times 4$ **q**-point mesh. These dynamic matrices in arbitrary wave vectors were evaluated using the Fourier convolution for these sets. Furthermore, the thermodynamic properties, including the specific heat capacity (C_v) versus temperature, were calculated using the quasi-harmonic Debye model (QHA) [13].

An *ab-initio* pseudopotential method was used to perform total energy calculations for arbitrary crystal structures. With this method, we applied a small amount of strain to the equilibrium lattice, obtained the change in total energy, and then derived elastic constants with the help of this information. Elastic constants are defined as a functions of the deformation parameter (δ), what is proportional to the second-order coefficient within a polynomial harmony of total energy.

A cubic lattice has three independent elastic constants: C_{11}, C_{12} and C_{44}. Thus, three equations are necessary to determine these constants.

$$B = (C_{11} + 2C_{12})/3 \,, \tag{1}$$

$$\overline{\varepsilon} = \begin{pmatrix} \delta & 0 & 0 \\ 0 & \delta & 0 \\ 0 & 0 & (1+\delta)^{-2} - 1 \end{pmatrix} \,, \tag{2}$$

$$\overline{\varepsilon} = \begin{pmatrix} \delta & \delta/2 & 0 \\ \delta/2 & 0 & 0 \\ 0 & 0 & \frac{\delta^2}{(4-\delta)^2} \end{pmatrix} \,. \tag{3}$$

Equation (1) calculates the bulk modulus (B), which depends on the values of C_{11} and C_{12} [14,15]. Hence, B can be obtained from $\frac{\Delta E}{V} = \frac{9}{2} B\delta^2$, where V is the volume of mesh cells without a force while ΔE is the energy change caused by an applied strain.

Equation (2) (tetragonal shear modulus) includes the volume-conserved tetragonal strain to determine $C_{11} - C_{12}$. This strain provides energy change, $\Delta E = 3V_o\ (C_{11} - C_{12})\delta^2 + \mathrm{O}\ [\delta^3]$. Equation (3) includes the strain volume- conserved base-centered orthorhombic strain tensor.

This strain provides energy change, $\Delta E = 1/2 C_{44} V o \delta^2 + \mathrm{O}\ [\delta^4]$. This energy change directly gives the value of C_{44}, and the value of C_{11} and C_{12} are calculated by combining the tetragonal shear modulus associated with the bulk modulus in Eq. (1). The elastic constants of X_2ScAl (X = Ir, Os, and Pt) compounds in the $L2_1$ phase were examined as functions of the hydrostatic pressure

Table 1. Lattice constants (a_0, Å), bulk moduli (B, GPa), elastic constants (C_{ij}, GPa) and Cauchy's pressure (CP) of X_2ScAl (X = Ir, Os, and Pt) in the $L2_1$ phase.

Material	Ref.	a_0	B	C_{11}	C_{12}	C_{44}	CP = $(C_{12} - C_{44})$
Ir_2ScAl	The present study	6.248	195.665	292.527	147.235	117.456	29.779
	Ref. 5	6.249	194	334	121	108	13
	Ref. 7	6.238					
Os_2ScAl	The present study	6.268	194.260	261.908	160.436	102.312	58.124
	Ref. 6	6.239					
	Ref. 7	6.244					
Pt_2ScAl	The present study	6.406	156.489	164.802	152.332	72.151	80.181
	Ref. 5	6.399	150	173	139	39	100
	Ref. 6	6.425					
	Ref. 7	6.389					

by calculating the bulk modulus (B) and two different shear moduli ($C' = (C_{11} - C_{12})/2$ and C_{44}) at various volumes. Details the elastic-constant calculation method are reported in previous studies [16–19].

The rigidity of a material is described as its ability to withstand elastic deformation, which can be defined by the bulk modulus (B) or the shear modulus (G). For a cubic structure, the shear modulus (G) can be calculated by using the following equations:

$$G_V = \frac{C_{11} - C_{12} + 3C_{44}}{5},$$
$$G_R = \frac{5(C_{11} - C_{12})C_{44}}{3(C_{11} - C_{12}) + 4C_{44}}$$
$$\text{and } G = \frac{G_V + G_R}{2}. \quad (4)$$

Here, G_V is the Voigt module while G_R is the Reuss module. While obtaining the Young modulus (E), one can obtain the relationship between the bulk modulus (B) and the shear module (G) from $= \frac{9BG}{3B+G}$. Poisson's ratio, which defines the volume change during uniaxial distortion, is obtained using the $\sigma = \frac{1}{2}\left(1 - \frac{E}{3B}\right)$. The anisotropy factor A was calculated using $A = \frac{2C_{44}}{(C_{11}-C_{12})}$.

III. RESULTS AND DISCUSSION

In the $L2_1$ phase, X_2ScAl (X = Ir, Os, and Pt) compounds have a cubic structure in the $Fm\bar{3}m$ (# 225) space group, as shown in Fig. 1. Here, X atoms are positioned at 8*c* (0.25, 0.25, 0.25), Sc atoms at 4*b* (0.5, 0.5, 0.5) and Al 4*a* (0, 0, 0) at the "Wyckoff" positions. In Table 1, the values of the calculated equilibrium lattice constant a_0 and the bulk modulus B of X_2ScAl (X = Ir, Os, and Pt) compounds are given in comparison with the data available in the literature. When the results calculated in the present study are compared with

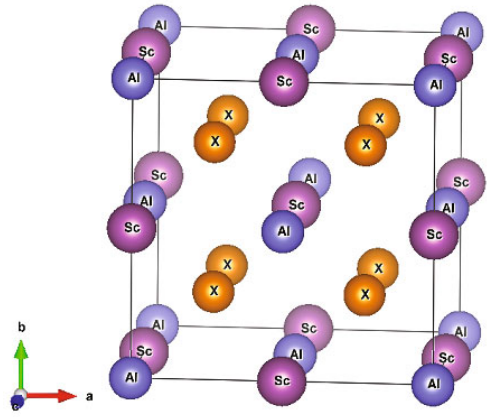

Fig. 1. Crystal structure of X_2ScAl (X = Ir, Os and Pt) compounds in the $L2_1$ phase.

the values found in the literature, the values are found to be very close to one another [5–7]. The lattice constants for Ir_2ScAl, Os_2ScAl, and Pt_2ScAl deviated approximately by 0.16%, 0.38% and 0.23%, respectively, from those reported in Ref. 16. No experimental values were found in the data available for lattice constants of the three compounds. The bulk modulicalculated for the compounds Ir_2ScAl and Pt_2ScAl were found to be close to the available theoretical results [5]. For the bulk modulus of Os_2ScAl, no comparable value was found in the literature.

Elastic constants require information on the energy derivative as a function of lattice strain. In the case of a cubic system, only three independent elastic constants, C_{11}, C_{12}, and C_{44}, exist the well-known "Born" stability criteria [20] are a set of conditions on elastic constants (C_{ij}) related to the second-order change in the internal energy of a crystal under deformation. The requirement for mechanical stability in a cubic crystal leads to the

Table 2. Bulk moduli (B, GPa) and Shear modulus (G, GPa) with subscripts R and V based on the Reuss and the Voigt averages, B/G ratios, Young's moduli (E), anisotropy factors (A) and Poisson's ratios (σ for X_2ScAl (X = Ir, Os, and Pt) compounds with $L2_1$ structures.

Material	Ref.	B	G_v	G_R	G	B/G	E	A	σ
Ir_2ScAl	The present study	195.665	99.532	94.215	96.871	2.019	249.426	1.616	0.28
	Ref. 5	194			107	1.813			0.27
Os_2ScAl	The present study	194.260	81.681	72.736	81.681	2.398	214.922	2.016	0.31
Pt_2ScAl	The present study	156.489	45.784	13.798	29.791	5.185	82.680	11.571	0.38
	Ref. 5	150			28	5.357			0.41

following limitations in elastic constants:

$$C_{44} > 0\ , \frac{(C_{11} - C_{12})}{2} > 0$$
$$\text{and } B = (C_{11} + 2C_{12})/3 > 0\ . \qquad (5)$$

The elastic constants calculated in this study are presented in Table 1. The elastic constants obtained for Ir_2ScAl are in line with the theoretical results of previous research [5]. Whereas the values of C_{11} and C_{12} were found to be compatible with the results obtained for Pt_2ScAl, the value of C_{44} was smaller than the previous theoretical result [5]. No findings were found in the available data for the compound Os_2ScAl. As the calculated elastic constants meet the mechanical stability conditions of the X_2ScAl (X = Ir, Os, and Pt) compounds considered, we concluded that these materials were mechanically stable. Comparing the C_{11} values of the compounds studied, we found that they were sorted as Ir_2ScAl, Os_2ScAl and Pt_2ScAl from high value to low volues. Thus, these materials are listed in descending order as Ir_2ScAl, Os_2ScAl, and Pt_2ScAl. Cauchy's pressure) (CP, where CP = $C_{12} - C_{44}$) [17] characterizes the predominant binding in the crystal. A negative value of CP shows a strong covalent bond while a positive value of CP indicates a strong metallic bond. The CP values for the three materials examined here were positive, and the most stable compound was Ir_2ScAl. These values confirm the metallic bond character of all three compounds; the calculated electronic band structures and the previously reported results [5] also confirm this result. In addition, the calculated bulk modulus, shear modulus (mean, Reuss and Voit values), Young's modulus, the anisotropy factor, Poisson's ratio, and the B/G ratio are presented in Table 2. Comparing the bulk and the shear moduli, we see that for all three compounds the bulk modulus was higher than the shear modulus. Accordingly, all three compounds should be able to resist changes in their volumes under pressure. Comparing the bulk moduli of the three materials, the abilities of Ir_2ScAl and Os_2ScAl to resist volume changes were found to be higher than that of Pt_2ScAl.

According to Pugh's [21] criteria, if the B/G Ratio is higher than 1.75, the materials are ductile; otherwise, the materials are brittle. The B/G values calculated for all three materials were higher than 1.75. Therefore, all three materials had a ductile nature, and this result confirmed previous data [5]. The rigidness of the compounds can be compared using the Young modulus. A higher Young modulus indicates a higher deformation resistance. Comparing the three compounds, we find the Ir_2ScAl compound to be the most robust with Young's modulus of 249.426 GPa whereas Pt_2ScAl was the least robust with a Young's modulus of 82.680 GPa. As shown in Table 2, the bulk, Young and shear moduli appeared to have the same tendencies, and all of these values were higher for Ir_2ScAl. Another datum based on the calculations of the elastic constants is the micro-hardness parameter (H). The magnitude of the micro-hardness is given by $H = [(1-2\sigma)E]/6(1+\sigma)$. The calculated H values were 14.290 GPa for Ir_2ScAl, 10.390 GPa for Os_2ScAl and 2.396 GPa for Pt_2ScAl. Information about the electronic properties of materials can be obtained by utilizing their elastic constants. According to the Pugh criteria, if Poisson's ratio is around 0.1, the material has a covalent bond while the material has an ionic bond when that ratio is around 0.25.

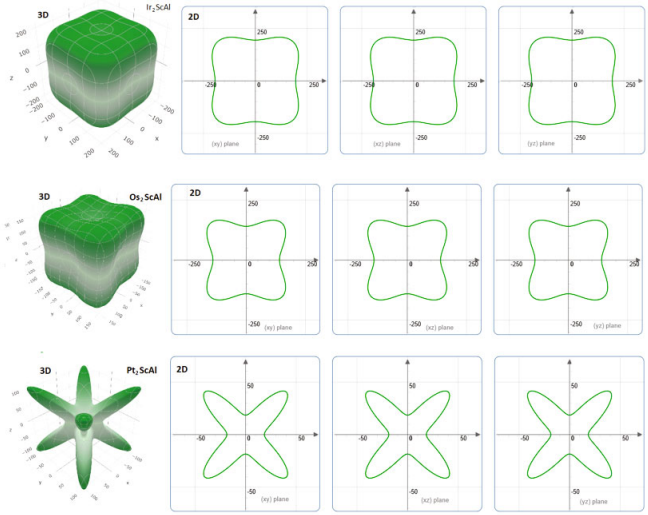

Fig. 2. Three-dimensional (3D) and two-dimensional (2D) directional dependence of the Young's moduli of X_2ScAl (X = Ir, Os and Pt) compounds in the $L2_1$ phase.

According to the Poisson ratios presented in Ta-

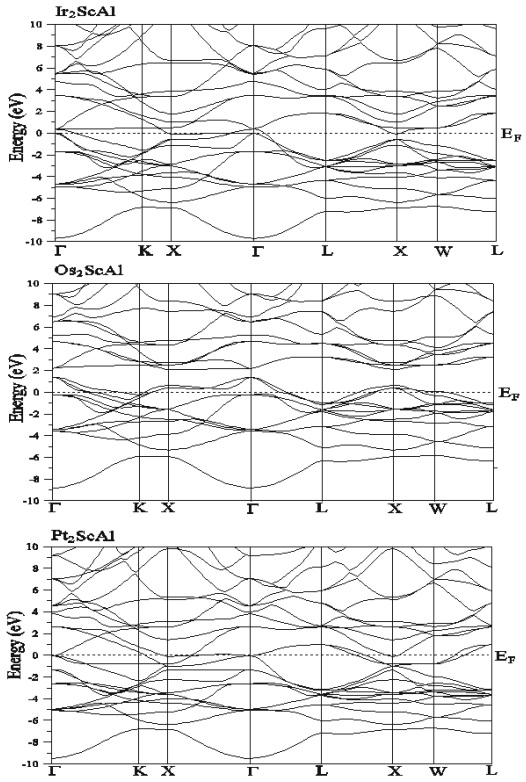

Fig. 3. Electronic band structures of X_2ScAl (X = Ir, Os and Pt) compounds in the $L2_1$ phase along the selected lines of high symmetry.

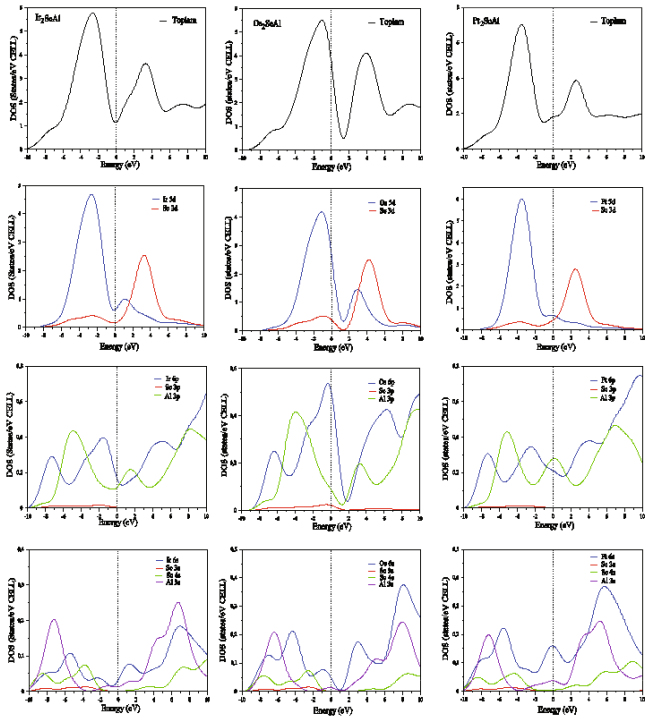

Fig. 4. Total and partial densities of states for X_2ScAl (X = Ir, Os and Pt) compounds in the $L2_1$ phase.

ble 2, all three compounds have ionic-metallic interactions. The anisotropy factor A is a measure of the degree of elastic anisotropy of a crystal. For a complete isotropic material, the anisotropy factor is 1, and the deviation from this value defines the degree of elastic anisotropy. According to the values presented in Table 2, the calculated anisotropy factors of the compounds were higher than 1; therefore, the compounds are elastically anisotropic. According to the data presented in Table 2, the compounds Ir_2ScAl, Os_2ScAl, and Pt_2ScAl have anisotropic properties. The Pt_2ScAl compound has the highest anisotropy. Both the two- and the three- dimensional directional dependences of the Young module were calculated by using the ELATE [22] package program for all materials, and the results are presented in Fig. 2. For an isotropic material, the shape is known to be spherical. The amount of deviation on the surfaces indicates the degree of anisotropy. As all the planes in Fig. 2 show, all three compounds are anisotropic, and Pt_2ScAl has the highest degree of anisotropy.

The electronic properties of X_2ScAl (X = Ir, Os, and Pt) compounds in $L2_1$ structure along the high symmetry directions are presented in Fig. 3. As Fig. 3 shows, the compounds do not have a band gap at the Fermi level because the valance and the conduction bands overlap significantly at the Fermi level. This showed that the compounds had a metallic character. In addition to the electronic band structure, Fig. 4 provides density of states graphs for a better understanding of the electronic contributions of these compounds. As Fig. 4 shows, all three materials had finite densities of states at the Fermi level. Therefore, no gap was found at the Fermi energy level, and the finite total densities of states were given as 1.1, 0.53 and 2.1 states eV^{-1} per unit cell for Ir_2ScAl, Os_2ScAl, and Pt_2ScAl, respectively. From Fig. 4, sharp peaks are seen above and below the Fermi level. The peaks around 3 eV for all three compounds were associated with Sc 3*d* electronic states. The large peak just below the Fermi level for each compound was related to the electronic Ir 5*d* state for Ir_2ScAl, the electronic Os 5*d* state for Os_2ScAl and the electronic Pt 5*d* for state Pt_2ScAl. The main contribution to the Fermi level in the three compounds was from Ir 5*d* (Os 5*d* and Pt 5*d*) and Sc 3*d* electronic bands. No experimental or theoretical results are available in the literature to compare the electronic properties of X_2ScAl (X = Ir, Os, and Pt) compounds in the $L2_1$ phase. Thus, the electronic properties of these compounds are presented for the first time, to the best of our knowledge, in the present study.

Full phonon spectra and partial phonon densities of states for X_2ScAl (X = Ir, Os and Pt) compounds are presented in Fig. 5 and Fig. 6, respectively. The full phonon spectra of X_2ScAl (X = Ir, Os and Pt) compounds are shown in Fig. 5. Because of the presence of four atoms in a primitive cell of the X_2ScAl compounds with the $Fm\bar{3}m$ space group in the $L2_1$ phase, the phonon distribution curves exhibit 12 branches for any wave vec-

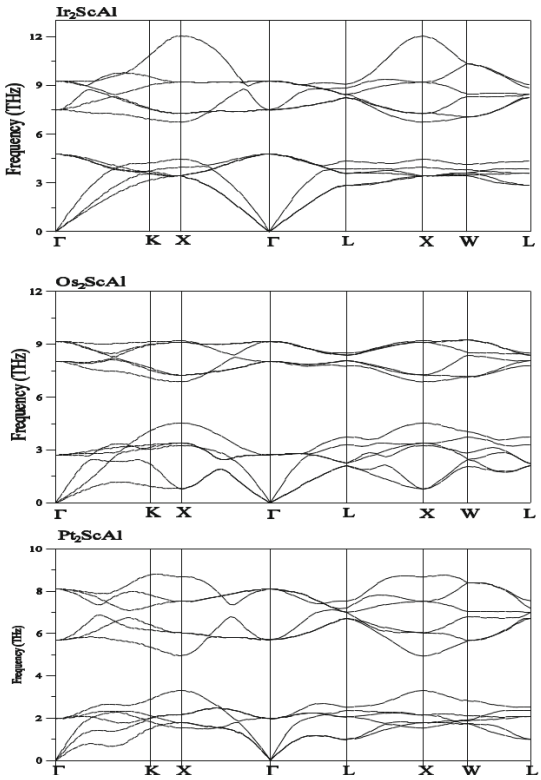

Fig. 5. Calculated phonon dispersion curves for X_2ScAl (X = Ir, Os and Pt) compounds in the $L2_1$ phase.

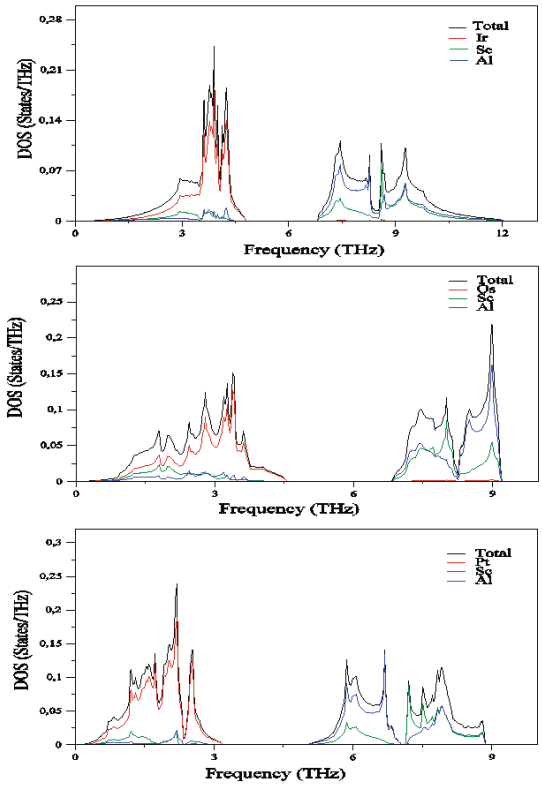

Fig. 6. Calculated total and partial phonon densities of states for X_2ScAl (X = Ir, Os and Pt) compounds in the $L2_1$ phase.

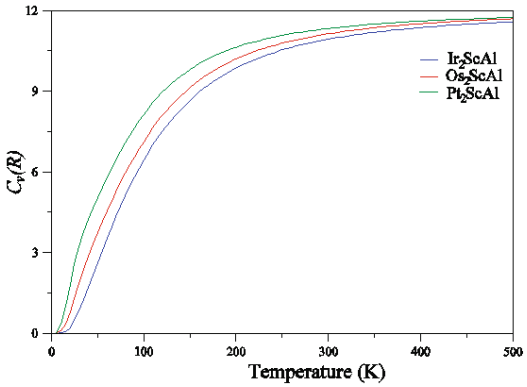

Fig. 7. Temperature dependences of the specific heat capacities at constant volume (CV) for X_2ScAl (X = Ir, Os and Pt) compounds.

tor: three acoustic and nine optical branches. X_2ScAl (X = Ir, Os and Pt) compounds are dynamically stable without any imaginary phonon frequencies in the entire Brillouin zone. The frequencies of the zone-center (Γ) phonon modes are of particular importance in the lattice dynamics of solids, because they can be analyzed by using different experimental techniques. The optical phonon frequencies at the zone-center (Γ) are 4.767, 7.504, and 9.271 THz for Ir_2ScAl; 2.761, 7.985 and 9.184 THz for Os_2ScAl; 2.012, 5.692 and 8.118 for Pt_2ScAl, respectively. Band gaps exist between the lower optical mode and the upper optical modes in all three compounds, as can be seen clearly in both Fig. 5 and Fig. 6. The computed band gap values are 1.91 THz for Ir_2ScAl, 2.279 for Os_2ScAl and 1.791 THz for Pt_2ScAl, respectively. As Fig. 6 shows, the heavier masses of Ir, Os and Pt cause the lower optical and the acoustic modes to overlap whereas the considerably lower masses of Sc and Al leads to separation of other upper optical branches from lower optical modes. The phonon band gaps can lead to several applications, such as sound filters and mirrors, because the gap sound does not spread and only a reflection from the surface exists [23]. This type of property make these materials ideal for use in both insulators and mirrors.

The specific heat capacity at constant-volume (C_v)-temperature relations for the X_2ScAl compounds are presented in Fig. 7. As Fig. 7 shows, the specific heat capacity C_v exponentially increases from 0 K to 500 K. The specific heat capacity C_v (T) as a function of temperature is close to a constant value at high temperature, which is called Dulong-Petit boundary, and sharply increases from 0 to 200 K. Argaman *et al.* [24] investigated the possible effects of the phonon band gap on the heat capacity. They suggested that a low temperature anomaly may occur in the heat capacity. The anomaly increases with increasing magnitude of the frequency dif-

ference (phonon band gap) between the two frequencies. If the calculated band gap is around 3 THz, the anomaly can hardly be identified. As the phonon band gap increases to 13 THz, the anomaly becomes more pronounced. Because the computed phonon band gaps of the three compounds are lower than 3 THz, we observed no such anomaly.

IV. CONCLUSIONS

The electronic, mechanical, thermodynamic and phonon properties of Ir_2ScAl, Os_2ScAl and Pt_2ScAl compounds with $Fm\bar{3}m$ (# 225) space group in the $L2_1$ phase were calculated using density functional theory. Firstly, the lattice constants of the compounds in the $L2_1$ phase were obtained and compared with those in the literature. The calculated elastic properties showed that these compounds in the $L2_1$ phase were mechanically stable. In addition, the bulk, shear and Young's modulus, as well as Poisson's ratio for these compounds were interpreted.

According to the B/G ratio, all three compounds were found to have a ductile behavior. The Young's modulus analysis show that all three materials were rigid. These compounds were found to be incompressible, hard materials based on their bulk and shear moduli. The values of Poisson's ratio showed that the compounds had an ionic-metallic character. On the other hand, an analysis of the electronic structure revealed that all three compounds had a metallic character. The metallic band property of these materials was confirmed based on the values of the Cauchy pressure. The phonon dispersion curves, as well as the densities of states, for Ir_2ScAl, Os_2ScAl and Pt_2ScAl along the high-symmetry directions of the Brillouin zone were calculated using DFPT. The calculated phonon dispersion curves were found to be dynamically stable in the $L2_1$ structure in all three compounds without any imaginary phonon frequency. The results of the phonon calculations in the present study will lead experimental and theoretical studies in the future. Using the calculated phonon density of states, we used the Quasi-Harmonic approach to determine the specific heat capacity at constant volume for different temperatures. Finally, we calculated the changes in the specific heat capacities of these compounds at temperatures between 0 and 500 K.

REFERENCES

[1] F. Heusler, Verh. Dtsch. Phys. Ges. **5**, 219 (1903).
[2] C. S. Jiang *et al.*, J. Magn. Magn. Mater. **471**, 82 (2019).
[3] T. Graf, C. Felser and S. S. Parkin, Prog. Solid State Chem. **39**, 1 (2011).
[4] M. Gilleßen and R. Dronskowski, J. Comput. Chem. **30**, 1290 (2009).
[5] M. De Jong *et al.*, Sci. Data **2**, 150009 (2015).
[6] J. E. Saal *et al.*, JOM **65**, 1501 (2013).
[7] M. Gillessen, Massgeschneidertes und Analytik-Ersatz über die quantenchemischen Untersuchungen einiger ternärer intermet-allisher Verbindungen, Dissertation, Aachen, 2009.
[8] S. Baroni *et al.*, Quantum-ESPRESSO: open-source package for research in electronic structure, simulation, and optimization, code available from: https://www.quantum-espresso.org/, April 2019.
[9] J. P. Perdew, K. Burke and M. Ernzerhof, Phys. Rev. Lett. **77**, 3865 (1996).
[10] M. Methfessel and A. T. Paxton, Phys. Rev. B **40**, 3616 (1989).
[11] S. Baroni, P. Giannozzi and A. Testa, Phys. Rev. Lett. **58**, 1861 (1987).
[12] S. Baroni, S. de Gironcoli, A. Dal Corso and P. Giannozzi, Rev. Mod. Phys. **73**, 515 (2001).
[13] S. Baroni, P. Giannozzi and E. Isaev, Rev. Mineral. Geochem. **71**, 39 (2010).
[14] M. J. Mehl, Phys. Rev. B **47**, 2493 (1993).
[15] M. J. Mehl, J. E. Osburn, D. A. Papaconstantopoulos and B. M. Klein, Phys. Rev. B **41**, 10311 (1990).
[16] S. Q. Wang and H. Q. Ye, Phys. Status Solidi B **240**, 45 (2003).
[17] S. Al, N. Arıkan and A. İyigör, Zeitschrift für Naturforschung A **73**, 859 (2018).
[18] G. D. Yıldız *et al.*, Int. J. Mod. Phys. B **32**, 1850214 (2018).
[19] O. Örnek, A. İyigor and N. Arıkan, J. Fac. Eng. Archit. Gazi Univ. **32**, 377 (2017).
[20] M. Born and K. Huang, *Dynamical Theory of Crystal Lattices* (Clarendon, Oxford, 1954).
[21] S. F. Pugh, Philos. Mag. **45**, 823 (1954).
[22] R. Gaillac, P. Pullumbi and F. Coudert, J. Phys.: Condens. Matter **28**, 275201 (2016).
[23] R. M. Hornreich, M. Kugler, S. Shtrikman and C. Sommers, J. Phys. I France **7**, 509 (1997).
[24] U. Argaman, R. E. Abutbul, Y. Golan and G. Makov, Phys. Rev. B **100**, 054104 (2019).